Dual functions of anti-reflectance and surface passivation of the atomic layer deposited Al_2O_3 films on crystalline silicon substrates

Li Qiang Zhu[a], Xiang Li, Zhong Hui Yan, Hong Liang Zhang, and Qing Wan[b]

Ningbo Institute of Materials Technology and Engineering, Chinese Academy of Sciences, Ningbo 315201, People's Republic of China

Surface anti-reflectance and passivation properties of the Al_2O_3 films deposited on crystalline Si substrates by atomic layer deposition are investigated. Textured Si with 100 nm Al_2O_3 shows a very low average reflectance of ~2.8 %. Both p-type and n-type Si wafers are well passivated by Al_2O_3 films. The maximal minority carrier lifetimes are improved from ~10 μs before Al_2O_3 passivation to above 3 ms for both p-type and n-type Si after Al_2O_3 passivation layer deposition and annealing at an appropriate temperature. Our results indicate the dual functions of anti-reflectance and surface passivation in c-Si solar cell applications.

[a] E-mail address: lqzhu@nimte.ac.cn

[b] Corresponding author. E-mail address: wanqing@nimte.ac.cn

Al_2O_3 thin films are of interest for various applications such as high-k gate candidates [1], protective coatings for a wide range of chemicals [2], optical waveguides [3], etc. Recently, Al_2O_3 have been received tremendous interest in the photovoltaic community due to their effective surface passivation to improve the efficiency. Ultra thin Al_2O_3 layers deposited on photoanodes used in dye-sensitized solar cells prevents the back recombination between electrons and the photoanodes, resulting in the improved cell efficiency. [4] Surface passivation of CIGS with atomic layer deposited (ALD) Al_2O_3 is also demonstrated due to the field shielding effects. [5] Al_2O_3 thin films provide excellent surface passivation on both lightly and highly doped p- and n-type crystalline silicon surfaces, resulting in the improved efficiency [6-10], which is due to the low density of interface defects D_{it} in the range of $10^{11}cm^{-2}eV^{-1}$ as well as a field effect passivation with a high density of fixed negative charges Q_{fix} above $10^{12}cm^{-2}$. [6, 11] To active the passivation, an annealing step at moderate temperatures after deposition was reported to be essential.[12]

At the same time, effective anti-reflective plays an important role for solar cells efficiency improvement. Conventionally, textured Si surface coated with SiN_x anti-reflective layer from production line shows an average reflectance of below 5%. It is reported [13] that the reflective index of Al_2O_3 thin films is ~1.6 at wavelength of 630nm, indicating that it is suitable for anti-reflectance applications in c-Si solar cells. Though the Al_2O_3 films have been widely employed to passivate the c-Si surface with a thickness below 50nm, the anti-reflective properties of Al_2O_3 films have not been reported yet. In this letter, both the anti-reflectance properties and the passivation

properties of the thermal ALD Al_2O_3 have been studied. A minimal reflectance of ~2.8 % was addressed. A maximal minority carrier lifetime of 4.7 ms and 3.4 ms were obtained for Al_2O_3 passivated p-Si and n-Si wafers, respectively. Such results indicate the dual functions of anti-reflectance and surface passivation in c-Si solar cell applications.

Commercially available single crystalline, 380μm-thick (100)-oriented p-type Czochralski (CZ) silicon wafers and 400μm-thick (100)-oriented n-type Czochralski (CZ) silicon were used as the substrates. For the anti-reflective testing, the wafers were textured by NaOH solution. Then the substrates underwent an HCl solution dip for 5min followed by a dilute HF dip. A de-ioned water rinse was adopted after each chemical dip steps. The Al_2O_3 films were deposited on the textured wafer for anti-reflectance studies by a thermal NCD 200B ALD reactor. To test lifetime, an Al_2O_3 film was deposited on both sides of the shiny-etched wafer to obtain symmetric lifetime sample. The stoichiometric Al_2O_3 films were deposited at 200℃ with a 100sccm background flow of N_2. A cycle in the reactor consisted of a 0.3s injection of $Al(CH_3)_3$ vapors followed by 7s N_2 purge. The oxidation step consisted of a 0.1s injection of H_2O vapor followed by a 7s purge with N_2 resulting in a deposition rate of 1.25 Å/cycle. 800, 560, and 240 ALD cycles were adopted on the textured p-type CZ silicon wafers for anti-reflectivity testing. While 800 and 240 ALD cycles were adopted on the CZ silicon wafers for lifetime testing. Control samples are also prepared on the shiny-etched p-type CZ silicon wafers received HF-last rinse to measure the film thickness by spectroscopy elliposometry. The post-deposition

annealing was performed in a quartz furnace at different temperature in atmosphere ambient.

The total spectral reflectance was measured by AudioDev's Helios LAB-rc system. Reflected light from a broadband halogen light source is collected and detected by a special designed integrating sphere. Therefore, all reflected or scattered light will be measured. Microwave photoconductance decay lifetime measurements were carried out to determine the passivation quality on a Semilab WT-2000PVN lifetime tester with excess carriers generated by a 200 ns laser pulse at a wavelength of 904 nm and a spot size of 1mm^2. The effective minority carrier lifetime τ_{eff} depends on both the bulk minority carrier lifetime τ_{bulk} and the surface recombination velocity S_{eff}.[14]

$$\frac{1}{\tau_{eff}} = \frac{1}{\tau_{bulk}} + \frac{2S_{eff}}{W}$$

where S_{eff} is the surface recombination velocity and W is the wafer thickness. S_{eff} is calculated from the effective minority carrier lifetime of the samples, considering their intrinsic lifetime values. The bulk minority carrier lifetime was assumed to be infinite. Accordingly, the calculated S_{eff} value marks an upper limit to the effective surface recombination velocity.

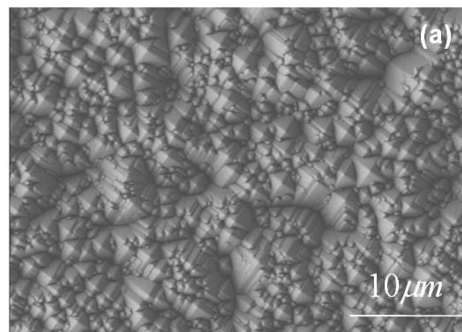

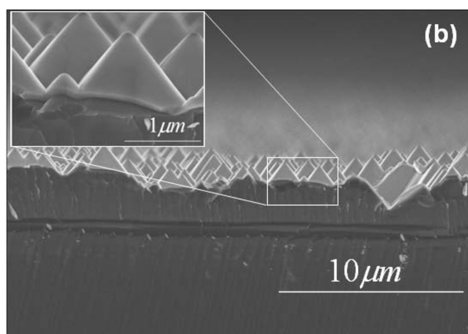

Fig.1 (a) SEM top view image of the Al_2O_3 coated textured Si surface of a (100)-oriented monocrystalline Si wafer after anisotropical wet chemical etching leaving (111) planes. (b) The micrograph of the cross-section of the Al_2O_3 coated textured Si.

A wet chemical alkaline anisotropically etching solution leads to the pyramidal surface topography. Fig.1 (a) shows the scanning electron microscopy (SEM) images of the surface morphology of the Al_2O_3 coated textured Si surface. (111) oriented Si crystal planes remain at the surface forming the pyramids. Fig.1 (b) shows a SEM cross section of a portion of the Al_2O_3 coated texture Si wafer. The thickness of the textured surface is estimated to be ~3 μm. An Al_2O_3 layer is obviously observed to be covered on the pyramids with the thickness of ~100 nm. Such textured surface helps to reduce the optical reflectance from 29.4% before texturing to 14.2% after texturing in average. While the Al_2O_3 over layer reduce the optical reflectance further, as will be discussed below.

Spectroscopic ellipsometry (SE) has been employed to investigate the optical characteristics of Al_2O_3 films. The thicknesses are determined to be ~100 nm, ~70 nm and ~30nm for 800, 560, and 240 ALD cycles, respectively. Fig.2 (a) presents the

refractive index (n) and extinction coefficients (k) of the as-deposited 100 nm Al_2O_3 in the wavelength range of 190 nm-1400 nm. The refractive index is measured to be ~1.65 at wavelength of 630 nm, similar to the reported value.[13] It is interesting to note that the extinction coefficient is determined to be close to zero for wavelength above 200nm. The absorption coefficients (α) could be obtained by a relationship, $\alpha=4\pi k/\lambda$, where λ was the wavelength of a photon as shown in Fig.2 (b). A significant increase of the absorption coefficient α at higher photon energy could be attributed to the band–band transitions. Since Al_2O_3 systems have an indirect fundamental gap, the interband absorption can be expressed by the following equation: [15]

$$\alpha h\upsilon \propto \left(h\upsilon - E_g\right)^2$$

where E_g is optical band gap energy. The inset in Fig.2 (b) illustrates the $(\alpha h\nu)^{1/2}$ *vs* photon energy ($h\nu$) curves. The linear behavior supports the interband transition. The extracted optical band gap (E_g) is ~6eV, which means that the deposited Al_2O_3 layer is transparent for the wavelength above 200 nm, ie, no absorption loss in the Al_2O_3 layer occurs for wavelength above 200 nm. The obtained results are meaningful for the anti-reflectance applications in solar cells.

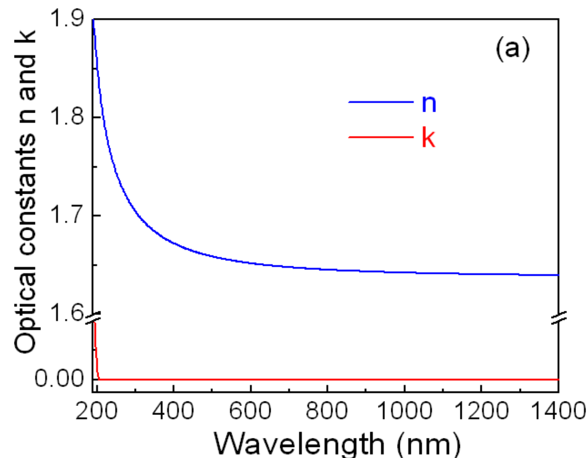

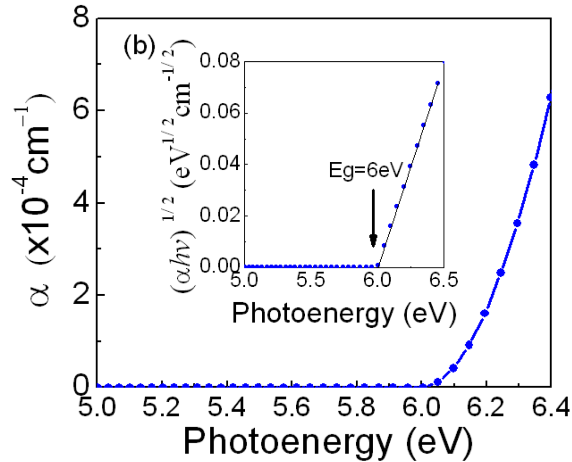

Fig.2 (a) Optical constants n and k for the as-deposited ~100 nm Al_2O_3 as a function of the wavelength obtained with spectroscopic ellipsometry measurements. (b) α vs *hv* plot of as-deposited 100 nm Al_2O_3 films. The inset figure shows the $(\alpha hv)^{1/2}$ vs *hv* plot. The intersection indicates the E_g value.

Fig.3 (a) illustrates the photographs of the textured Si coated with 100 nm, 70 nm and 30 nm Al_2O_3, showing the best anti-reflectance properties for 100 nm Al_2O_3 coated textured Si. Photographs for textured Si and SiN_x coated textured Si are included as references. Fig.3 (b) shows the reflectance spectrum of the Al_2O_3 coated textured Si wafers with different Al_2O_3 thickness. Reflectances for the textured Si and the SiN_x coated textured Si are also included for comparison. The standard SiN_x coated textured Si are obtained from the production line, noted as standard (STD) sample. The average reflectance is ~14.2 % for the textured Si. It decreases to ~10.6 % and ~4.2 % when depositing ~30 nm Al_2O_3 and ~70 nm Al_2O_3, respectively. Meaningfully, the reflectance spectra for ~100 nm Al_2O_3 coated textured Si are quite similar to that of the STD sample. At the low wavelength, the reflectance for ~100 nm

Al_2O_3 is a little higher than the STD sample, while at the higher wavelength, the reflectance is a little lower than the STD sample, which results in the best reflectance of ~2.8 % for ~100 nm Al_2O_3 on the textured Si, close to 2.9 % for the STD sample. The results indicate the potential anti-reflectance applications of Al_2O_3 in c-Si solar cells.

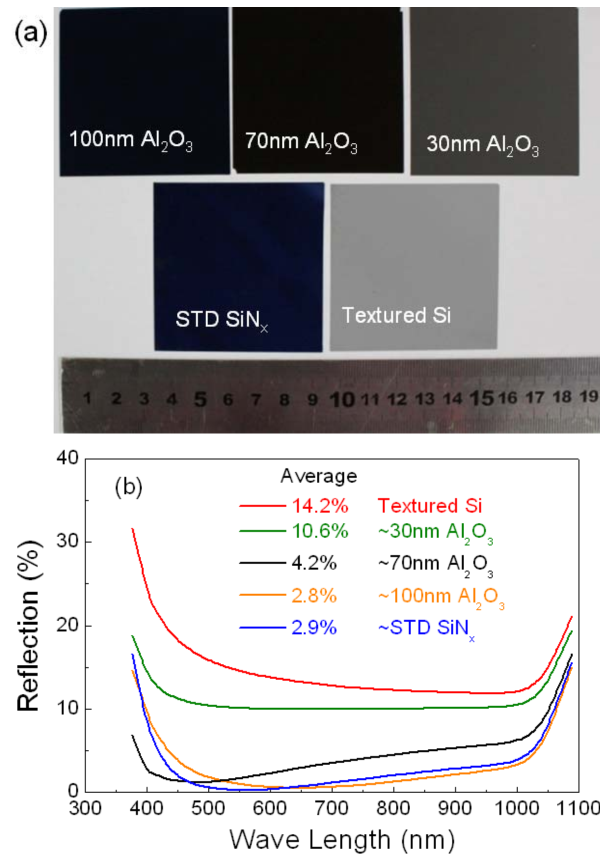

Fig.3 (a) A photograph of the texture Si coated with 100nm, 70nm, 30nm Al_2O_3 and STD SiN_x. Textured Si as the reference. (b) Reflectance curves for the Al_2O_3 coated textured Si. Results for the textured Si and standard SiN_x coated textured Si (STD SiN_x) are included for comparison.

Independent of the deposition method, a post-deposition anneal is necessary to

activate the passivating properties of Al_2O_3. Fig.4 illustrates the effective carrier lifetime (Fig.4 (a)) and the surface recombination velocity (Fig.4 (b)) of p-type CZ Si wafers as a function of the applied thermal treatment for 30 nm and 100 nm Al_2O_3 coated Si. For the original Si wafer, a low lifetime of ~6 μs is obtained. After depositing a 100 nm-thick Al_2O_3 layers, a moderate surface passivation level has been addressed, yielding an effective lifetimes τ_{eff} of ~140 μs, similar to what has been observed for conventional thermal ALD.[16] While depositing a 30 nm-thick Al_2O_3 layers results in a high effective lifetimes τ_{eff} of ~910 μs. To study the full potential for the surface passivation and the thermal stability of the Al_2O_3 layers deposited in this work, the lifetime samples were exposed to a post-deposition annealing in atmosphere ambient for 5 min with temperature ranging from 300 ℃ to 650 ℃. A flash annealing was also performed at 900 ℃ for 3 s. For the 100 nm Al_2O_3 coated lifetime samples, annealing performed at 600 ℃ for 5 min yields a good passivation with the lifetime of ~750 μs. While for the 30nm Al_2O_3 coated lifetime samples, a best passivation is obtained at 350 ℃ with a lifetime of ~4.7 ms. Annealing the sample at higher temperature results in the deteriorated lifetime. The flash annealing for 30nm Al_2O_3 coated lifetime samples at 900 ℃ for 3 s yields a moderate level of surface passivation with lifetime of 120 μs.

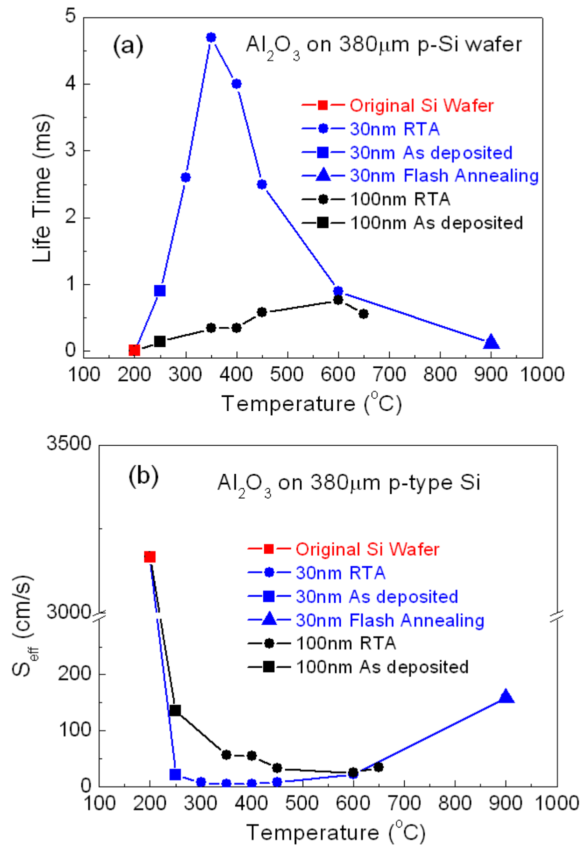

Fig.4 (a) Life time values for p-type Si passivated by 100 nm and 30 nm Al_2O_3. (b) Effective surface recombination velocity (S_{eff}).

The upper limit of the effective surface recombination velocity was also calculated as shown in Fig.4 (b). For the original Si wafer, a high S_{eff} value of ~3170 cm/s is determined. The deposition of 100 nm Al_2O_3 layer results in a moderate S_{eff} of ~130 cm/s, while the deposition of 30nm Al_2O_3 results in a low S_{eff} of ~20 cm/s. The post-deposition annealing treatment results in the improved S_{eff}. For 100 nm Al_2O_3 coated Si wafers, the best results are obtained at 600 ℃, yielding a lowest S_{eff} of ~25cm/s. While for 30 nm Al_2O_3 coated Si wafers, a very low S_{eff} <20 cm/s is obtained. The lowest S_{eff} of ~4 cm/s is addressed at 350 ℃. The flash annealing at

900 ℃ for 3s yields a moderate level of surface passivation with S_{eff} of 160 cm/s, respectively.

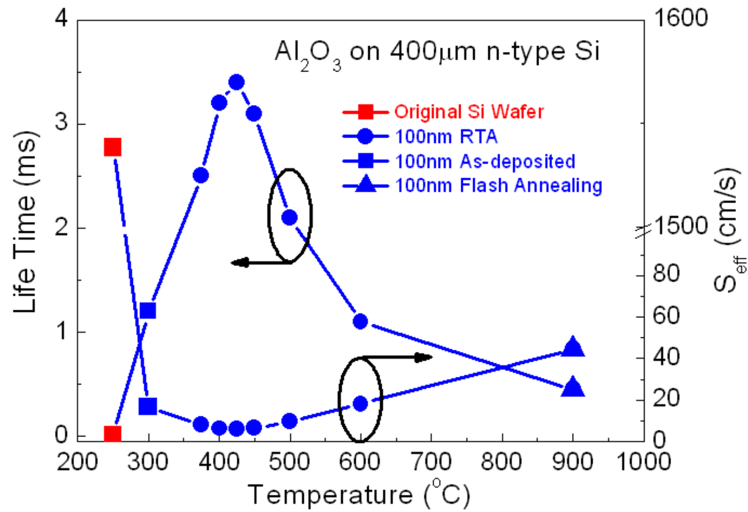

Fig.5 Life time values for n-type Si passivated by 100 nm Al_2O_3 and the effective surface recombination velocity (S_{eff}).

Similarly, n-type Si wafers are also passivated by 100 nm thick Al_2O_3, as shown in Fig.5. For the original Si wafer, a low lifetime of ~13 μs is obtained. After passivating with a 100 nm thick Al_2O_3, the effective minority carrier lifetime increased to 1.2 ms and 3.4 ms for the as-deposited sample and the 425 ℃ annealed sample, repectively. The flash annealing at 900 ℃ for 3 s yields a moderate level of surface passivation with lifetime of 450 μs. The upper limit of the effective surface recombination velocity is obtained. For the original Si wafer, a high S_{eff} of ~1540 cm/s is determined. The deposition of 100 nm Al_2O_3 layer results in a low S_{eff} of ~16 cm/s. The lowest S_{eff} of ~6 cm/s is addressed at 425 ℃. The flash annealing at 900 ℃ for 3s yields a moderate level of surface passivation with S_{eff} of 44 cm/s, respectively.

The activation of the passivation are attributed to a strong field effect passivation caused by a high negative fixed charge density in the Al_2O_3 films located close to the interface.[11] While the deteriorating of the passivation at the higher temperature would be attributed to the deteriorated interface properties, ie, the increased D_{it} and the defects density.

In summary, Al_2O_3 layers were deposited by thermal ALD on p-type and n-type CZ Si wafers. The textured Si coated with 100nm Al_2O_3 shows a low average reflectance of ~2.8 %. Both p-type and n-type Si wafers are well passivated by Al_2O_3 films. The maximal minority carrier lifetimes are improved from ~10 μs before Al_2O_3 passivation to above 3 ms for both p-type and n-type Si after Al_2O_3 passivation and annealing. Our results indicate the dual functions of anti-reflectance and surface passivation in c-Si solar cell applications.

Acknowledgement

Programs supported by Ningbo Natural Science Foundation (2011A610202), and the National Natural Science Foundation of China (11104288).

References

[1] L.Q.Zhu, N.Barrett, P.Jegou, F.Martin, C.Leroux, E.Martinez, H.Grampeix, O.Renault, and A.Chabli, J.Appl.Phys. **105**, 024102 (2008).

[2] M.M.Şovar, D.Samélor, A.Gleizes, P.Alphonse, S.Perisanu, and C.Vahlas, Advanced Materials Research, **23**, 245 (2007).

[3] M.M.Aslan, N.A.Webster, C.L.Byard, M.B.Pereira, C.M.Hayes, R.S.Wiederkehr, and S.B. Mendes, Thin Solid Films, **518**, 4935 (2010).

[4] C.Prasittichai and J.T.Hupp, J.Phys.Chem.Lett. **1**, 1611 (2010).

[5] W.-W.Hsu, J.Y.Chen, T.-H.Cheng, S.C.Lu, W.-S.Ho, Y.-Y.Chen, Y.-J.Chien, and C.W.Liu, Appl. Phys. Lett. **100**, 023508 (2012).

[6] F.Werner, B.Veith, V.Tiba, P.Poodt, F.Roozeboom, R.Brendel, and J.Schmidt, Appl. Phys. Lett. **97**, 162103, (2010).

[7] N.M.Terlinden, G.Dingemans, M.C.M.Van de Sanden, and W.M.M.Kessels, Appl.Phys.Lett. **96**, 112101 (2010).

[8] B.Hoex, M.C.M.Van de Sanden, J.Schmidt, R.Brendel, and W.M.M.Kessel, Phys.Status Solidi RRL, **6**, 4 (2012).

[9] B.Vermang, H.Goverde, L.Tous, A.Lorenz, P.Choulat, J.Horzel, J.John, J.Poortmans, and R.Mertens, Prog. Photovolt: Res.Appl. **20**, 269 (2012)

[10] H.Lee, T.Tachibana, N.Ikeno, H.Hashiguchi,K.Arafune, H.Yoshida, S-I.Sato, T.Chikyow, and A.Ogura, Appl.Phys.Lett., **100**, 143901 (2012)

[11] B.Hoex, J.J.H.Gielis, M.C.M.Van de Sanden, and W.M.M.Kessels, J.Appl.Phys. **104**, 113703 (2008)

[12] J.Benick, A.Richter, T.T.A.Li, N.E.Grant, K.R.McIntosh, Y.Ren, K.J.Weber, M.Hermle, and S.W.Glunz Proceddings of 35th IEEE Photovoltaic Specialists Conference, Honolulu, Hawaii, 2010, p.891.

[13] P.Saint-Cast, D.Kania, M.Hofmann, J.Benick, J.Rentsch, and R.Preu, Appl.Phys.Lett., **95**, 151502 (2009).

[14] B.Hoex, J.Schmidt, P.Pohl, M.C.M.Van de Sanden, and W.M.M.Kessels, J.Appl.Phys. **104**, 044903 (2008).

[15] L.Q.Zhu, Q.Fang, X.J.Wang, J.P.Zhang, M.Liu, G.He, and L.D.Zhang, Appl.Surf.Sci. **254**, 5439 (2008)

[16] G.Dingemans, R.Seguin, P.Engelhart, M.C.M.van de Sanden, and W.M.M.Kessels, Phys.Status Solidi (RRL) **4**, 10 (2010)